Cloning and Expression Analysis of *AzanOBP7*, a Minus-C Odorant-Binding Protein Gene, from *Agrilus zanthoxylumi* (Coleoptera: Buprestidae)[1]

Xiao-Jin Gao[3], Li Guo[3,4], Na Jiang, Yu Qi, Qin-Yao Jin, Shou-An Xie[2], and Shu-Jie Iv

Northwest A&F University, Yangling, Shaanxi, 712100, China

J. Entomol. Sci. 58(4): 447–459 (October 2023)
DOI: 10.18474/JES22-68

Abstract Odorant-binding proteins (OBPs) play an important role in specific recognition, binding, and transportation of odorants. In this study, the full-length complementary DNA (cDNA) sequence of *AzanOBP7*, a Minus-C OBP gene, from *Agrilus zanthoxylumi* Li Ming Lou (Coleoptera: Buprestidae) was cloned by rapid amplification of cDNA ends based on transcriptome data. The bioinformatic analysis showed that *AzanOBP7* contains a 450-bp open reading frame encoding a 149-residue polypeptide, with a molecular mass of 17.176 kDa. It was predicted to be a nontransmembrane protein with an 18–amino acid signal peptide at the N terminus. The predicted three-dimensional structure of AzanOBP7 by AphadFold2 possesses seven α helices and two disulfide bridges. The multiple sequence alignment and phylogenetic tree revealed that *AzanOBP7* reached the highest identity (94.70%) with *Agrilus mali* Matsumura (Coleoptera: Buprestidae) AmalOBP11; they also were closely aligned in a clade. Quantitative real-time polymerase chain reaction showed that *AzanOBP7* exhibited the highest expression level in the abdomen of adult females. In the thorax, the expression level in adult males was significantly higher than that in other aged males ($P < 0.01$). Our study offers a theoretical foundation for further study on the functional characteristics of *A. zanthoxylumi* OBPs.

Key Words *Agrilus zanthoxylumi*, *AzanOBP7*, clone, bioinformatic analysis, tissue expression

Agrilus zanthoxylumi Li Ming Lou (Coleoptera: Buprestidae) is a serious trunk borer of Chinese prickly ash (*Zanthoxylum nitidum* (Roxburgh) de Candolle), with a distribution mainly in northern China (Dang 1988, Li. et al. 1990). *Agrilus zanthoxylumi* undergoes complete metamorphosis, with larvae and adults being the stages that are harmful to Chinese prickly ash. In the larval stage, *A. zanthoxylumi* consumes phloem cells 10–40 cm above the ground, resulting in hollow breakage of plant phloem (Xu et al. 2020). Gradually, they begin to feed on the cambium, and the injured parts of Chinese prickly ash exude a mixture of white and yellow foam and water. Adults feed on leaves and females lay eggs under the bark, resulting in nicks and holes in the foliage or softening, decaying, and cracking of the bark (Du 2012, Gao and Zhang 2007, Wang et al. 2012).

[1]Received 5 December 2022; accepted for publication 2 February 2023.
[2]Corresponding author (email: shouanxie@163.com).
[3]Co–first authors who contributed equally to this study and manuscript.
[4]Liaoning Provincial Saline-Alkali Land Utilization and Research Institute, Panjin, LiaoNing, 124000, China.

The olfactory system of insects plays an important role in many physiological and behavioral activities, such as finding suitable hosts, food, oviposition sites, and mating partners (Breer 2003). It consists of various proteins, odorant-binding proteins (OBPs), chemosensory proteins (CSPs), odorant-degrading enzymes, odorant receptors, gustatory receptors, ionotropic receptor, and sensory neuron membrane proteins (Vosshall et al. 1999). As a carrier, OBPs can bind to specific odorants in the environment and transport them to the corresponding receptors (Kaissling 2009, Laughlin et al. 2008, Vogt and Riddiford 1981, Xu et al. 2005). The function of OBPs to specifically recognize odorants has been verified in Lepidoptera, Coleoptera, Hemiptera, Hymenoptera, and Orthoptera (Li et al. 2019, Sun et al. 2020).

OBP is a small water-soluble protein with a relative molecular mass of 13∼17 kDa (Ahmed et al. 2017). According to the number and site of cysteine (Cys) in OBPs, they can be divided into five types: Classic OBP with six Cys, Plus-C OBP with a conserved proline site behind the sixth Cys, Dimer OBP with two Cys, Minus-C OBP with four or five Cys, and Atypical OBP with two domains identical to classic OBP (Fan et al. 2011). According to the previous measure of insect OBPs' gene expression in different tissues, most OBP genes are specifically or abundantly expressed in the insect antennae. There are also some OBP genes expressed in other tissues or organs with nonolfactory functions. *CsupOBP1* is highly expressed in the head of *Chilo suppressalis* (Walker) (Lepidoptera: Crambidae) larvae and in the tarsi and wings of adults (Wei et al. 2013). It is speculated that *CsupOBP1* is involved in regulating oviposition by females on the leaves of host plants. Expression of OBPs in the gonads of *Aedes aegypti* (L.) (Diptera: Culicidae) *AipsOBP6* may be related to the dissemination of sex pheromones after their release as well as the process of female moths' (Lepidoptera) detecting their own release of sex pheromones (Gu et al. 2013). These results indicate that AzanOBP7 may be involved in nonolfactory functions in *A. zanthoxylumi*, with differences between males and females in these functions.

In this study, polymerase chain reaction (PCR) and rapid amplification of complementary DNA (cDNA) ends (RACE) were used to clone *AzanOBP7* of *A. zanthoxylum*, a Minus-C OBP gene. Its sequence and structural characteristics were also analyzed. Quantitative real-time (qRT)-PCR was used to examine the relative expression levels of the *AzanOBP7* gene in different tissues and sexes of *A. zanthoxylumi*. Our results establish a foundation for further research on the function of OBPs and olfactory mechanisms.

Materials and Methods

Insects. Adults of *A. zanthoxylumi* were collected from the wild in Puhua Town, Lantian County, Xi'an Municipality, Shaanxi Province, China, in June 2020. The captured adults were placed in 5-ml centrifuge tubes, fed with Chinese prickly ash leaves, and then transported to the laboratory where adult males and females were separated according to morphological characteristics. Specimens were dissected to yield head, thorax, abdomen, tarsus, and wing tissues from both sexes, and these structures were stored at −80°C until used for analyses.

Isolation of RNA and synthesis of first-strand cDNA. Total RNA for identification and tissue expression pattern of the *AzanOBP7* gene was extracted from

Table 1. Primers for amplification of full-length complementary DNA (cDNA) and quantitative real-time polymerase chain reaction (qRT-PCR).

Name*	Primer sequence (5′–3′)	Use
AzanOBP7-F	GGAGTGAGTCTGAACGTGATAG	Amplification of midpart sequence
AzanOBP7-R	TGTGTTTTCTCCTCTTCTTCCG	
5-GSP	CCCTAGAATTACCAGAAGATGATCC	5′ rapid amplification of cDNA ends (RACE)
5-NGSP	TCTATCAC GTTCAGACTCACTCC	
3-GSP	TATACGAAAAGGGGTTATCAAAATGA	3′ RACE
3-NGSP	CCCCAAAACGGAAGAAGAGG	
AzanOBP7X-F	ATGGATCCTGGTAAGTCTAACACTATCGAA	Amplification of coding sequence
AzanOBP7X-R	ACTTTCCTGGGTTTTCTCTTCCTCTTCCG	
AzanOBP7q-F	CCTAGAATTACCAGAAGATGAT	qRT-PCR
AzanOBP7q-R	CTTCAGGTGTTGTTCCTT	
28S-F	GAAAATGAGTCCGAGGCAAAA	
28S-R	TAAAACAGGAAGTGGTGAGGC	

* OBP, odorant-binding protein; GSP, Gene specific primers; NGSP, Nested gene specific primers; F, forward; R, reverse.

both sexes and five tissues of *A. zanthoxylumi* by using TRIzol reagent (BTN81220, Biolab, Beijing, China). The extraction of total RNA was conducted in accordance with the manufacturer's instructions. The integrity of RNA was measured by 1.5% agarose gel electrophoresis, and the purity and concentration of RNA samples were detected using a NanoDrop™ 2000 spectrophotometer (Thermo Fisher Scientific, Waltham, MA) to ensure that the A_{260}/A_{280} was between 1.8 and 2.0. The first-strand cDNA was synthesized by reverse transcription reaction using cDNA and a first-strand reverse transcription kit (R133-01, Vazyme, Beijing, China) with random primers.

Molecular cloning of full-length cDNA of the *AzanOBP7* gene. According to the transcriptome data of the *AzanOBP7* gene (SUB6796283), primers for amplifying the midpart sequence of the *AzanOBP7* gene were designed using Primerl SGD (https://www.yeastgenome.org/primer3?result=1; accessed 12 June 2022), with AzanOBP7-F as the forward primer and AzanOBP7-R as the reverse primer (Table 1). The 25-μl PCR reaction volume included 1 μl of cDNA template, 12.5 μl of 2× Es Taq Master Mix, 1 μl of forward primer, 1 μl of reverse primer, and 9.5 μl of double distilled water. The PCR was performed under the following conditions: 94°C for 3 min, 35 cycles of 94°C for 30 s, 56°C for 30 s, and 72°C for 1 min, and an extension at 72°C for 5 min.

For RACE, gene-specific primers and nested gene-specific primers were designed for 5′ and 3′ RACE based on confirmed midpart sequence by using

Primer|SGD (Table 1). The 5′ and 3′ ends of *AzanOBP7* gene were amplified according to the manufacturer's instructions for the SMARTer RACE 5′/3′ kit (634858, TaKaRa, Beijing, China). Finally, the full-length cDNA of the *AzanOBP7* gene was determined by assembling three regions including the midpart, 3′ end, and 5′ end of the *AzanOBP7* gene by using DNAMAN 9.0.

The coding sequence (CDS) was determined based on the assembled full-length cDNA of the *AzanOBP7* gene. For the amplification of CDS, its process can refer to the amplification process of the midpart sequence by using AzanOBP7X-F as the forward primer and AzanOBP7X-R as the reverse primer.

The PCR products were separated by 1.5% agarose gel electrophoresis and stained with GoldView dye. The band of the expected size was excised and purified using a gel extraction kit (D2500-02, OMEGA, Beijing, China). The purified bands were cloned into a pMD18-T cloning vector (6011, TaKaRa) and then transformed into DH5α competent cells (B528413, Sangon Biotech, Beijing, China). Successful clones were sent to Shanghai Biotechnology Services Co., Ltd. (Shanghai, China) for sequencing.

Sequence analysis and phylogenetic tree construction. The open reading frame (ORF) of the *AzanOBP7* gene was predicted using the online tool ORFfinder (https://www.ncbi.nlm.nih.gov/orffinder/; accessed 12 June 2022). The amino acid sequence encoded by the CDS was deduced by DNAMAN, the molecular mass and isoelectric point were determined and analyzed by ExPASy-ProtParam tool (https://web.expasy.org/protparam/; accessed 12 June 2022), and the signal peptide of the amino acid sequence was predicted by SignalP (http://www.cbs.dtu.dk/services/SignalP/; accessed 12 June 2022).

OBPs with high similarity to AzanOBP7 were searched through the National Center for Biotechnology Information BlastN search program (https://blast.ncbi.nlm.nih.gov/Blast.cgi; accessed 12 June 2022). A multiple sequence alignment was performed with ClustalX software. The phylogenetic tree was constructed by MEGA7.0 software by using neighbor-joining method, supported by 1,000-fold bootstrap resampling.

Modeling and evaluation. The AlphaFold2 was used to predict the three-dimensional (3D) model of AzanOBP7. The modeling was performed based on the primary amino acid sequence removing signal peptides.

The three modules ProCheck, Verification-3D, and ERRAT3 in SAVES, Version 6.0 online tool (https://saves.mbi.ucla.edu/, accessed 22 June 2022) were used to evaluate the rationality of AzanCSP7 protein model, and PROSA online tool (https://prosa.services.came.sbg.ac.at/prosa.php; accessed 22 June 2022) was used to evaluate the quality of the model. Finally, we performed model alignment of AzanCSP7 and *Apis mellifera* L. (Hymenoptera: Apidae) AmelOBP14 by using the PyMOL software.

qRT-PCR. qRT-PCR was used to examine the relative transcription levels of the *AzanOBP7* gene in different tissues and sexes of *A. zanthoxylumi*. The primers of qRT-PCR were designed using Primer3|SGD (https://www.yeastgenome.org/primer3; accessed 5 July 2022), AzanOBP7q-F as the forward primer, and AzanOBP7q-R as the reverse primer (Table 1). The assay was performed on a Bio-Rad PCR instrument using the QuantiNova SYBR Green PCR kit (208054, Qiagen, Hilden, Germany) in a total volume of 20 μl, including 10 μl of 2× Taq SYBR Green qPCR Mix, 0.4 μl of AzanOBP7X-F, 0.4 μl of AzanOBP7X-R, 1 μl of

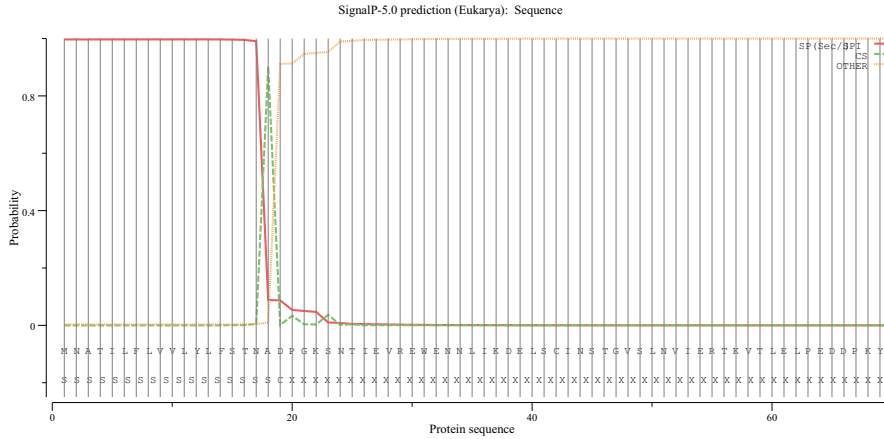

Fig. 1. Signal peptide of AzanOBP7 predicted by SignalP-5.0.

template cDNA, and 8.2 μl of nuclease-free water. The *28S* gene served as the internal control. Thermal cycling conditions were as follows: a holding step at 95°C for 3 min, followed by 40 cycles of 95°C for 20 s, 50°C for 30 s, and 72°C for 30 s. To detect and validate the specific of amplification products, melting curve analysis from 55 to 95°C was used to the end all reactions. There were three technical and three biological replicates for each sample. The relative expression level of *AzanOBP7* gene was calculated by the $2^{-\triangle\triangle Ct}$ method.

Results

Sequence analysis of *AzanOBP7* and phylogenetic tree construction. The full-length cDNA sequence of *AzanOBP7* gene (GenBank ID: MT318836) was successfully cloned; its length was 921 bp. The ORF of the *AzanOBP7* gene consisted of 450 nucleotides that encoded 149 amino acids. The 5′ untranslated region and 3′ untranslated region was 283 and 179 bp, respectively. The predicted signal peptide of the deduced protein contained 18 amino acids (Fig. 1). AzanOBP7 had a calculated isoelectric point of 4.85 and molecular mass of 17.176 kDa. The transmembrane prediction by using the hidden Markov models (TMHMM) program result showed that AzanOBP7 has no transmembrane domain (Fig. 2).

Based on multiple sequence alignment, the AzanOBP7 most closely identified (94.7%) with *Agrilus mali* Matsumura (Coleoptera: Buprestidae) AmalOBP11. The identity between AzanOBP7 with OBPs of other coleopterans tested was relatively low, ranging from 61.7 to 45.7%. The result showed that AzanOBP7 possesses four conserved Cys residues, matching the pattern of Minu-C OBPs: X_{42}-C_1-X_{30}-C_2-X_{37}-C_3-X_{19}-C_4-X_{12}, where X = any amino acid (Fig. 3).

A phylogenetic tree of AzanOBP7 and OBPs from other coleopterans was constructed by the neighbor-joining method. AzanOBP7 and AmalOBP11 were closely aligned in a clade (Fig. 4), and the other OBPs formed another clade, the former and the latter belonging to Minus-C OBP and Classic OBP, respectively.

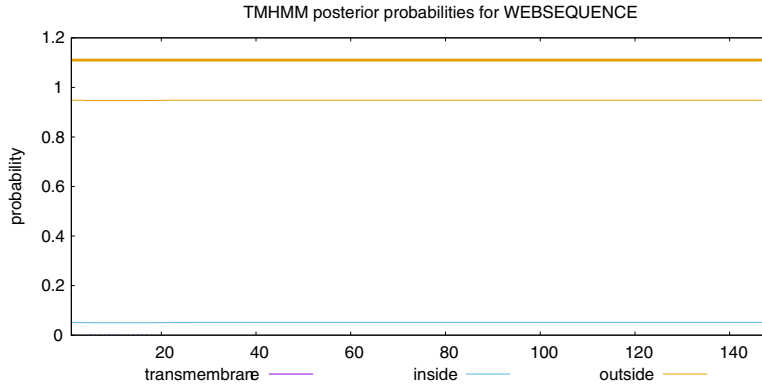

Fig. 2. Transmembrane domain of AzanOBP7 analyzed by transmembrane prediction by using the hidden Markov models (TMHMM) program.

Spatial structural analysis of AzanOBP7. The 3D structure of AzanOBP7 was successfully simulated with AlphaFold. The Ramachandran plot showed that 96.6% of the AzanOBP7 residues are in the most favored regions, 2.5% are in additional allowed regions, 0.8% are in generously allowed regions, and none are in the disallowed region (Fig. 5), indicating that the predicted 3D structure is acceptable and reliable. Analysis by the PROSA program shows that the *Z* score value is −5.34 (Fig. 6), which is within the *Z* score distribution of favorable structural proteins. Through analysis by Verify3D, 84.73% of residues averaged a 3D-1D score ≥0.2 (Fig. 7), showing that the model is of high quality. Statistics of amino acids by using

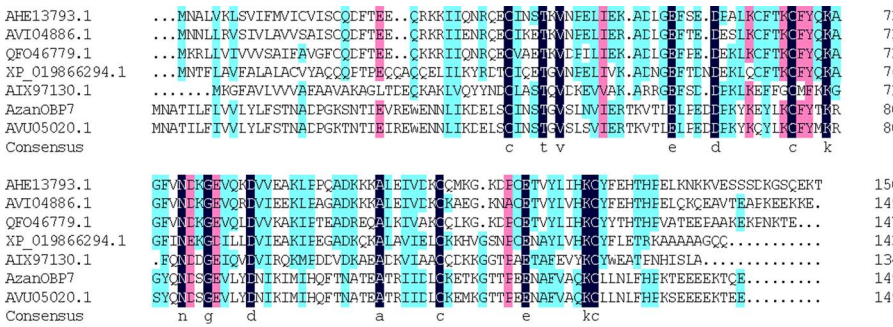

Fig. 3. Multiple sequence alignment among AzanOBP7 with OBPs from various coleopterans. Black, pink, blue, and white represent completely identity, identity above 75%, identity above 50%, and identity below 30%, respectively. GenBank ID and its corresponding odorant-binding protein (OBP): AHE13793.1 (*Lissorhoptrus oryzophilus* OBP), AVI04886.1 (*Cylas formicarius* putative OBP 5), QFO46779.1 (*Cylas formicarius* OBP), XP019866294.1 (*Aethina tumida* general OBP 56d-like isoform X2), AIX97130.1 (*Rhyzopertha dominica* OBP 7), AVU05020.1 (*Agrilus mali* OBP 11).

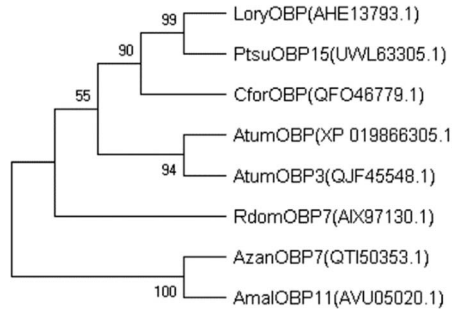

Fig. 4. Phylogenetic tree of AzanOBP7 and odorant-binding proteins (OBPs) from various coleopterans. GenBank ID and its corresponding OBP: AHE13793.1 (*Lissorhoptrus oryzophilus* OBP), UWL63305.1 (*Pagiophloeus tsushimanus* OBP 15), QFO46779.1 (*Cylas formicarius* OBP), XP019866305.1 (*Aethina tumida* general OBP 56d-like), QJF45548.1 (*Aethina tumida* OBP 3), AIX97130.1 (*Rhyzopertha dominica* OBP 7), QTI50353.1 (*Agrilus zanthoxylumi* OBP 7), AVU05020.1 (*Agrilus mali* OBP 11).

the ERRAT program showed that the ERRAT value is 98.3471% (Fig. 8), a value much higher than 50%, indicating that the noncovalent bond interaction in AzanCSP7 model was reasonable as a whole.

The predicted 3D structure of AzanOBP7 consists of seven α helices: α1 (Val10 to Thr28), α2 (Leu32 to Val40), α3 (Pro49 to Lys61), α4 (Tyr73 to Gln82), α5 (Ala86 to Lys97), α6 (Pro104 to Leu118), and α7 (His120 to Thr129) (Fig. 9). Two disulfide bridges (D1 and D2) were observed (Cys24 in α1 and Cys57 in α3, Cys96 in α4 and Cys114 in α6). It can be seen from the model alignment that both have seven helixes, and the position and size of helixes in AzanCSP7 and AmelOBP14 are almost identical, except for the helix in the C-terminal; the helix in the C-terminal extends in two different directions (Fig. 10).

Expression of *AzanOBP7* in tissues (head, thorax, abdomen, tarsus, and wing) of male and female adults. *AzanOBP7* was expressed ubiquitously in all the examined tissues including head, thorax, abdomen, tarsus, and wing of both sexes of *A. zanthoxylumi*. *AzanOBP7* showed the highest expression level in the abdomen of adult females. The expression level of *AzanOBP7* in the abdomen and leg of both sexes did not differ significantly ($P > 0.05$). In the head and wing, the expression level in adult females was significantly higher than that in adult males ($P < 0.05$). In the thorax, the expression level in adult males was significantly higher than that in adult females ($P < 0.01$).

Discussion

The full-length cDNA of the *AzanOBP7* gene was successfully cloned and is the first Minus-C OBP gene identified from *A. zanthoxylumi*. Compared with the pattern of Classic OBPs, C_1-X_{20-66}-C_2-X_3-C_3-X_{21-43}-C_4-X_{8-14}-C_5-X_8-C_6, there are only four conserved Cys residues of AzanOBP7, and Cys in the second and fifth positions are

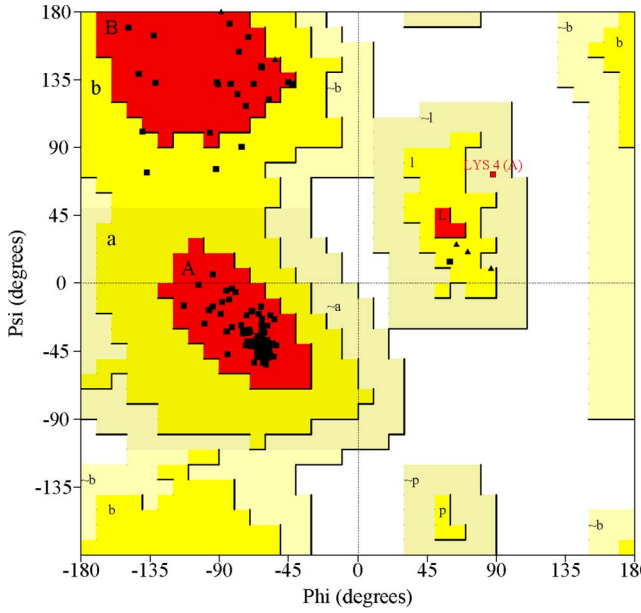

Fig. 5. Ramachandran plot of AzanOBP7 model. Letter and its corresponding residues are as follows: [A, B, L], residues in most favored regions; [a, b, l, p], residues in additional allowed regions; [~a, ~b, ~l, ~p], residues in generously allowed regions. Region without letters represents residues in disallowed regions.

replaced by other amino acids. The Minus-C OBP subfamily has been reported in some insects, such as *Monochamus alternatus* Hope (Coleoptera: Cerambycidae) (Zhang et al. 2020), *Helicoverpa armigera* (Hübner) (Lepidoptera: Noctuidae) (Zhao et al. 2013), *Microplitis mediator* (Haliday) (Hymenoptera: Braconidae) (Zhang et al. 2009), and *Apis mellifera* (Forêt and Maleszka 2006). Disulfide bonds between Cys residues play an important role in advanced structure and stability of OBPs (Pelosi and Maida 1995): more disulfide bonds may make the structure more complex to meet the requirements for identification of specific odorants. Previous studies on the evolutionary histories of chemosensory systems showed that Classic-C OBPs might originate from Minus-C OBPs.

AzanOBP7 most closely identified (94.70%) with AmalOBP11, and both proteins formed a close clade in the constructed phylogenetic tree (e.g., bootstrap value = 100%). Previous research found that AmalOBP11 also belongs to Minus-C OBPs (Cui 2018). It is speculated that the two genes may be differentiated from the same gene and highly conserved through evolution. Furthermore, through examining the expression level of the *AzanOBP7* gene, it was found that *AzanOBP7* has the highest expression in nonolfactory tissues and the abdomen of female *A. zanthoxylumi*, followed by high expression in the abdomen of males. The expression level was relatively low in the head, chest, tarsus, and wing of both sexes. The expression of *AmalOBP11* in the abdomen of females was significantly higher than

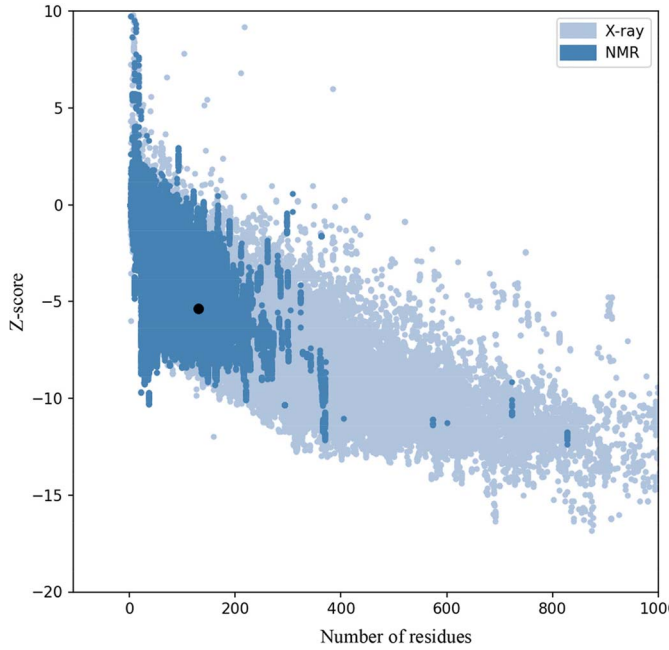

Fig. 6. Z score of AzanOBP7 model. In this plot, groups of structures from different sources (X-ray, nuclear magnetic resonance) are distinguished by different colors.

that in antennae and other tissues (Cui 2018). The results showed that the expression of *AzanOBP7* in the abdomen is similar to that of *AmalOBP11*. We speculate that AzanOBP7 and AmalOBP11 do not participate in olfactory perception and may be related to the secretion and release of sex pheromone by females (Paolo et al. 2018).

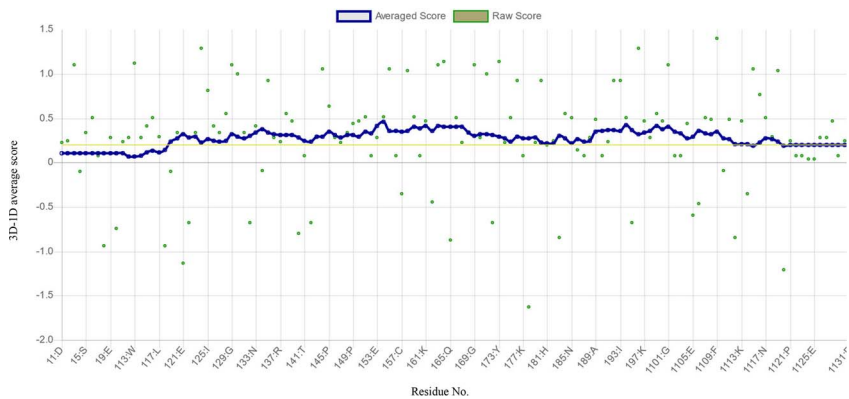

Fig. 7. Verify-3D scores of AzanOBP7 model.

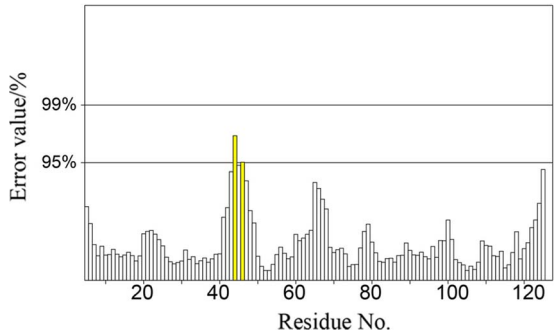

Fig. 8. Error values of AzanOBP7 model residues.

The Swiss model workspace was used to simulate the 3D structure of AzanOBP7, but the consistency with the template was >30%. Therefore, AlphaFold2 was used for modeling. Using the latest CASP13 competition that assesses the ability of methods to predict novel protein folds, AlphaFold2 was first used in the Free Modeling category (Ivanov et al. 2022). AzanOBP7 possesses seven α helices and two disulfide bridges, similar to the 3D structure of AmelOBP14 (Silvia et al. 2011) and belongs to Minus-C OBPs; AmelOBP14 possesses a core of six α helices, comparable with that of Classic OBPs, and an extra exposed C-terminal helix characterized by only two disulfide bridges. But the helix in the C-terminal of AmelOBP14 and AzanOBP7 extends in two directions. The C-terminal side of different OBPs or the same protein in different states is variable; when binding and releasing odorant molecules, an OBP may adjust its conformation of C-terminal (Xu et al. 2010). It is speculated that AzanOBP7 and AmelOBP14 have different

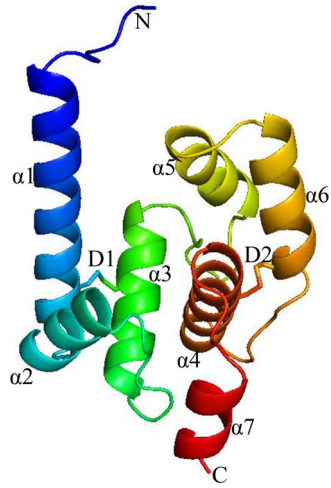

Fig. 9. Three-dimensional structure of AzanOBP7. The seven α helices are labeled as α1–α7. The two disulfide bonds are labeled as D1 and D2.

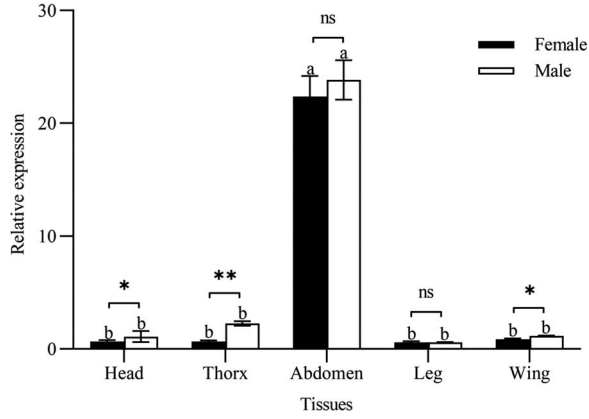

Fig. 10. Expression of *AzanOBP7* in tissues (head, chest, abdomen, foot, and wing) of adult males and females of *Agrilus zanthoxylumi*. Data are means ± SEM. The relative expression of AzanOBP7 in the same tissue of different sexes was analyzed by independent sample *t* test. ns, no significant difference ($P > 0.05$); *, significant difference ($P < 0.05$); **, highly significant difference ($P < 0.01$). The relative expression of AzanOBP7 in different tissues of the same sex was analyzed by one-way analysis of variance, and there was a significant difference between the relative expression of AzanOBP7 denoted by different letters ($P < 0.05$).

functions. The function of AzanOBP7 can be studied by site-directed mutagenesis, molecular docking, and fluorescence competitive binding in the future.

Acknowledgments

This study was supported by the "Development and application technology of pheromone attractant of *Agrilus zanthoxylum* in Lantian County" (2022JH-JSYF-0261) and "Shaanxi Province's Second Batch of Special Support Program Leading Talent Project." Mention of a commercial or proprietary product does not constitute an endorsement of the product by the Northwest Agriculture and Forestry University.

References Cited

Ahmed, T., T.T. Zhang, Z.Y. Wang, K.L. He and S.X. Bai. 2017. Molecular cloning, expression profile, odorant affinity, and stability of two odorant-binding proteins in *Macrocentrus cingulum* Brischke (Hymenoptera: Braconidae). Arch. Insect Biochem. Physiol. 94: e21374.

Breer, H. 2003. Sense of smell: Recognition and transduction of olfactory signals. Biochem. Soc. Trans. 31: 113–116.

Cui, X.N. 2018. Study on the behavioral response and olfactory related gene function of *Gideon applis* to host plant volatiles. PhD Dissertation. Northwest Agriculture and Forestry University, Yangling, China.

Dang, X. 1988. A primary study of three important pests of *Zanthoxylum simulans*. Shaanxi For. Sci. Technol. 2: 57–62.

Du, P. 2012. Study on occurrence and control of *Agrilus zanthoxylumi*. J. Green Sci. Technol. 8: 57–58.

Fan, J., F. Francis, Y. Liu, J.L. Chen and D.F. Cheng. 2011. An overview of odorant-binding protein functions in insect peripheral olfactory reception. Genet. Mol. Res. 10: 3056–3069.

Forêt, S. and R. Maleszka. 2006. Function and evolution of a gene family encoding odorant binding-like proteins in a social insect, the honey bee (*Apis mellifera*). Genome Res. 16: 1404–1413.

Gao, H.T. and G.L. Zhang. 2007. Biological characteristics and integrated control measures of *Agrilus zanthoxylumi*. Shaanxi J. Agric. Sci. 2: 183–184.

Gu, S.H., K.M. Wu, Y.Y. Guo, J.A. Pickett, L.M. Field, J.J. Zhou and Y.J. Zhang. 2013. Identification of genes expressed in the sex pheromone gland of the black cutworm *Agrotis ipsilon* with putative roles in sex pheromone biosynthesis and transport. BMC Genomics 14: 636.

Ivanov, Y.D., A. Taldaev, A.V. Lisitsa, E.A. Ponomarenko and A.I. Archakov. 2022. Prediction of monomeric and dimeric structures of CYP102A1 using AlphaFold2 and AlphaFold multimer and assessment of point mutation effect on the efficiency of intra- and interprotein electron transfer. Molecules 27: 1386.

Kaissling, K.E. 2009. Olfactory perireceptor and receptor events in moths: A kinetic model revised. J. Comp. Physiol. A Neuroethol. Sens. Neural Behav. Physiol. 195: 895–922.

Laughlin, J.D., T.S. Ha, D.N.M. Jones and D.P. Smith. 2008. Activation of pheromone-sensitive neurons is mediated by conformational activation of pheromone-binding protein. Cell 133: 1255–1265.

Li, L., Y. Tan, X.R. Zhou and B.P. Pang. 2019. Molecular cloning, prokaryotic expression and binding characterization of odorant binding protein gdauOBP20 in *Galeruca daurica*. Sci. Agric. Sin. 52: 3705–3712.

Paolo, P., I. Immacolata, J. Zhu, G.R. Wang and F.R. Dani. 2018. Beyond chemoreception: Diverse tasks of soluble olfactory proteins in insects. Biol. Rev. Camb. Philos. Soc. 93: 184–200.

Pelosi, P. and R. Maida. 1995. The physiological functions of odorant-binding proteins. Biophysics 40(1): 143–151.

Silvia, S., A. Lagarde, I. Iovinella, P. Legrand, M. Tegoni, P. Pelosi and C. Cambillau. 2011. Crystal structure of *Apis mellifera* OBP14, a C-Minus odorant-binding protein, and its complexes with odorant molecules. J. Insect Biochem. Mol. Biol. 42: 41–50.

Sun, Y.L., Q.H. Lv, H.B. Yang, Z.J. Hu, D.X. Li and J.F. Dong. 2020. Tissue expression profiling and ligand binding characterization of the Plus-C odorant binding protein PsauOBP7 of *Peridroma saucia*. Acta Entomol. Sin. 63: 807–816.

Vogt, R.G. and L.M. Riddiford. 1981. Pheromone binding and inactivation by moth antennae. Nature 293(5828): 161–163.

Vosshall, L.B., H. Amrein, P.S. Morozov, A. Rzhetsky and R. Axel. 1999. A spatial map of olfactory receptor expression in the *drosophila* antenna. Cell 96: 725–736.

Wang, Y., R.N. Li, X.T. Liu and N. Wang. 2012. The occurrence and control of *Agrilus zanthoxylumi* in HanCheng. J. Shaanxi For. Sci. Technol. 1: 76–77.

Wei, D., Z.F. Ye, J.Q. Gao and S.L. Dong. 2013. Molecular cloning and functional identification of *Chilo suppressalis* Minus-C odor binding protein. Acta Insectae Sin. 56: 754–764.

Xu, P.X., R. Atkinson, D.N.M. Jones and D.P. Smith. 2005. *Drosophila* OBP LUSH is required for activity of pheromone-sensitive neurons. Neuron 45: 193–200.

Xu, X.J., C.Z. Zhang, F. Li and T.B. Ru. 2020. Occurrence regularity and integrated control of the *Agrilus zanthoxylumi*. Northwest Gardening 2: 40–41.

Xu, X.Z., X. Wei, J. Rayo, Y. Ishida, W.S. Leal and J.B. Ames. 2010. NMR structure of navel orange worm moth pheromone-binding protein (AtraPBP1): Implications for pH-sensitive pheromone detection. Biochemistry 49: 1469–1476.

Zhang, F.M., M. Austin, Z.B. Zhao, Y.H. Zhang, J. Zhang, Q.W. Zhang, Q.H. Wang, X.G. Zhou and X.R. Li. 2020. Characterization of MaltOBP1, a Minus-C odorant-binding protein, from the Japanese pine sawyer beetle, *Monochamus alternatus* Hope (Coleoptera: Cerambycidae). J. Front. Physiol. 11: 212.

Zhang, S.A., Y.J. Zhang, H.H. Su, X.W. Gao and Y.Y. Guo. 2009. Identification and expression pattern of putative odorant-binding proteins and chemosensory proteins in antennae of the *microplitis mediator* (Hymenoptera: Braconidae). Chem. Senses 34: 503–512.

Zhao, Q., S. Li, J.Y. Luo, J.J. Cui, Y. Ma and S.L. Dong. 2013. Two Minus-C odorant binding proteins from *Helicoverpa armigera* display higher ligand binding affinity at acidic pH than neutral pH. J. Insect Physiol. 59: 263–272.